Training effects in Gd_5Ge_4: role of microstructure

2006 J. Phys.: Condens. Matter 18 6017

(http://iopscience.iop.org/0953-8984/18/26/020)

INSTITUTE OF PHYSICS PUBLISHING JOURNAL OF PHYSICS: CONDENSED MATTER

J. Phys.: Condens. Matter **18** (2006) 6017–6032 doi:10.1088/0953-8984/18/26/020

Training effects in Gd_5Ge_4: role of microstructure

Meghmalhar Manekar[1], M K Chattopadhyay[1], R Kaul[2], V K Pecharsky[3,4] and K A Gschneidner Jr[3,4]

[1] Magnetic and Superconducting Materials Section, Raja Ramanna Centre for Advanced Technology, Indore 452 013, India
[2] Industrial CO_2 Laser Section, Raja Ramanna Centre for Advanced Technology, Indore 452 013, India
[3] Materials and Engineering Physics Program, Ames Laboratory, US DOE, Iowa State University, Ames, IA 50011-3020, USA
[4] Department of Materials Science and Engineering, Iowa State University, Ames, IA 50011-3200, USA

Received 18 January 2006, in final form 27 April 2006
Published 19 June 2006
Online at stacks.iop.org/JPhysCM/18/6017

Abstract

Detailed optical metallographic studies at room temperature on polycrystalline Gd_5Ge_4 are presented for two cases: (a) a sample in the as-cast condition and (b) the same sample subjected to a known number of temperature and magnetic field cycles. A herringbone- (criss-cross-) like pattern whose characteristic feature size extends to $\approx$20 μm is observed in the as-cast sample. The herringbone pattern at room temperature is interpreted as arising due to a long-lived (kinetically arrested) metastable phase. This herringbone pattern can be trained to form a pattern having a different morphology by cycling the sample through the low-temperature field induced magneto-structural transition. Training effects are also observed in magneto-transport and magnetization measurements as the sample is subjected to temperature and field cycles. Based on heuristic arguments, a model is proposed which self-consistently explains anomalies in transport and magnetization properties in terms of changes occurring in the microstructure of the sample. These results highlight the need for analysing the interesting properties of Gd_5Ge_4 and its family of alloys with microstructure as an important component.

(Some figures in this article are in colour only in the electronic version)

1. Introduction

Gd_5Ge_4 and other members of the $Gd_5(Si_xGe_{4-x})$ series have attracted considerable attention due to their giant magnetocaloric effect (MCE), colossal magnetostriction and giant magnetoresistance [1, 2]. Many compounds from the $Gd_5(Si_xGe_{4-x})$ series undergo a first

order magneto-structural transition (FOMST) driven by temperature (T) and/or magnetic field (H) either between paramagnetic (PM) and ferromagnetic (FM) states or between antiferromagnetic (AFM) and FM states depending on the value of x [2–4]. A structural transition which accompanies the magnetic transition makes this series of alloys attractive for potential use in magnetic refrigerators, as the isothermal entropy change due to the structural transformation may account for more than half of the observed MCE [5]. For a material to become technologically viable, the preparation and characterization details need to be standardized and considerable effort has been already expended to find the stable metallurgical phases of this series of alloys [4]. Since these materials undergo FOMST, it is also important to study the influence of quenched-in disorder on the FOMST process. It is known that random quenched-in disorder leads to broadening of the first order transition [6]. In this regard, the role of interstitial impurities present in Gd in determining the magnitude of the MCE [7, 8] and the extent of colossal magnetostriction [9] in the final product has been studied in detail. While all these efforts were focused on understanding the effects of removing or adding imperfections occurring at the atomic level due to chemical species, some effort has been carried out at micron length scales to study phase relationships and surface structure of the pure germanide—Gd_5Ge_4—and some of the Si doped alloys [10–13]. The focus of these surface measurements has mainly been to study the effect of preparation methods on the final chemical composition and phase segregation in these alloys.

Another aspect, which is important for a material to become practical, is that it should exhibit reproducible behaviour even after undergoing a large number of temperature, magnetic field or pressure cycles. The effect of repeated magnetic field and temperature cycling has been studied systematically and it is now known that the total electrical resistivity of these materials shows a monotonic increase when a sample is cycled through the FOMST [14–16]. This behaviour was interpreted as occurring due to additional cracks opening up [14] as the sample undergoes large volume changes across the FOMST. On the contrary, Sousa *et al* [16, 17] present some resistivity results which show a complex behaviour with cycling and thus apparently indicate that micro-cracking may be playing only a secondary role. There was also a conjecture that the Ge and Si atoms rearrange and give rise to a redistribution of the Si and Ge in the intra- and inter-layer sites along with a change in microstructure after prolonged cycling of the sample repeatedly through the FOMST [14]. In a recent study on $Gd_5Si_2Ge_2$, the presence of acoustic emission was demonstrated across the FOMST [18]. This acoustic activity was shown to approach a reproducible pattern after repeated thermal cycling through the FOMST. This evolution was shown to be analogous to the evolution seen in martensitic transitions [18].

In an attempt to answer some of the questions raised by various authors during their studies of the effect of repeated cycling through the FOMST, we performed a detailed metallographic examination of the pure Gd_5Ge_4 compound in connection with our magneto-transport study [19]. This end compound of the $Gd_5(Si_xGe_{4-x})$ series was chosen to avoid possible complications arising due to phase inhomogeneities during the interpretation of microstructures. Gd_5Ge_4 crystallizes in the Sm_5Ge_4 type orthorhombic structure (O(II)) [2], and orders antiferromagnetically at $T_N \approx 130$ K [15]. AFM order persists down to at least 2 K [20] in a zero magnetic field. At low temperatures, the AFM state can be transformed to the FM state with the application of magnetic field exceeding 1 T depending on the value of temperature (see [21] for a detailed H–T phase diagram). This AFM to FM transition can be brought about by applying hydrostatic pressure as well [22]. Through high resolution x-ray diffraction measurements, it was shown that the AFM to FM transition is accompanied by a structural change from the Sm_5Ge_4 type structure to the Gd_5Si_4 type orthorhombic

structure (O(I)) [5]. The AFM to FM transition is irreversible at temperatures below ≈10 K, partially reversible between 10 and 20 K and completely reversible at temperatures above ≈20 K [20, 21, 23]. Magnetic relaxation measurements highlighted the presence of metastable states across the FOMST and it was shown that for $T < 10$ K the back-transformation is arrested well beyond the experimentally accessible timescales [24].

While most of the efforts on Gd_5Ge_4 were focused on the origin and nature of the magnetic phase transitions, a systematic study relating the change in microstructure with the change in transport and magnetic properties is lacking. This work is one attempt in the direction of establishing such results. The microstructure was examined before the sample was subjected to magnetic-field and temperature cycling and then after passing it through the FOMST by a known number of temperature and magnetic field cycles. We find that the microstructural changes can be correlated with the changes in transport properties. Through an independent investigation we have found that the magnetization behaviour also exhibits training effects. In the following sections, we first summarize our results of metallographic, magneto-transport and magnetization measurements. Later we attempt to form a unified framework which explains these training effects in addition to showing that the role of microstructure is quite important in deciding the transport as well as magnetization properties of Gd_5Ge_4 and likely other members of this extended family of alloys.

2. Experimental details

A polycrystalline Gd_5Ge_4 button was made by arc melting the constituent elements, whose preparation and characterization details are given elsewhere [2]. Different pieces of the same button were used in other studies as well [5, 19, 24]. A sample suitable for metallography was cut in a rectangular shape of approximately 3 mm × 2 mm × 1.5 mm using an ISOMET® diamond wheel. The rectangular piece was polished through a sequence of grinding, coarse polishing (using TEXMET® polishing cloth and 4 μm diamond lapping compound) and fine polishing (using MICROCLOTH® and 0.5 μm diamond lapping compound). Polishing was done at very slow speeds (15–20 rpm) using an ISOMET® polishing unit. Due to the brittle nature of the sample, the polished surface shows many cracks when observed under a microscope. Instead of achieving mirror quality polish on the entire surface, individual islands enclosed by the cracks were monitored for the polishing quality. The polished sample surface was cleaned first with acetone and then with running water to remove the lapping compound and the lubricant. The sample was then etched at room temperature in a solution of 2% nitric acid by volume in methanol. The microstructure was observed using an OLYMPUS® microscope.

After the metallographic studies on the as-cast sample were completed, the sample was mounted for transport measurements which were performed using a commercial Oxford 16 T magnet cryostat system. The 3 mm × 2 mm surface of the sample was glued to a flat surface of a large copper block using GE varnish. A carbon-glass sensor was mounted in close proximity of the sample for measuring the temperature of the sample. Resistance measurements were made using a standard four-probe method. Electrical contacts were soldered to the sample with indium. Direct current was passed through the sample using a Keithley 224 current source and the voltage from the sample was measured using a Keithley 2182 nanovoltmeter. Once the transport measurements were completed, the sample was removed at room temperature and metallography measurements were performed on the same specimen.

An independent investigation using another piece of Gd_5Ge_4 extracted from the same batch was done to study the magnetization behaviour after repeated cycling through the FOMST. The magnetization (M) was measured using a SQUID magnetometer (Quantum Design MPMS-5).

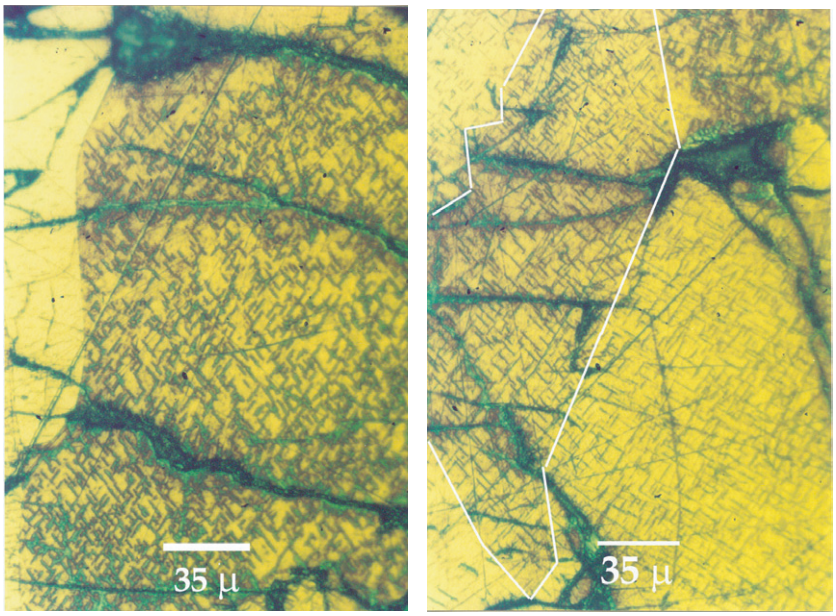

(a) (b)

Figure 1. Optical metallography of Gd_5Ge_4 revealing the criss-cross pattern seen at two different locations in the virgin sample. (a) Criss-cross pattern seen in only one grain of the two shown here. (b) Criss-cross pattern seen in adjacent grains. Note that the directionality of the linear features changes across the grain boundary. The white line marks the boundary between two adjacent grains.

3. Results

3.1. Microstructure of the as-cast sample

Figure 1 shows the microstructure at two different locations of the sample. A herringbone[5] (criss-cross) pattern appears in most of the grains (almost over the entire sample surface) when etching is continued for about 150 s. Figure 1(a) shows one location where the criss-cross pattern is revealed in one grain while the adjacent grain does not show any such pattern. Similar linear features have been seen before in the pure Gd_5Ge_4 compound and the Si doped compound as well [10–13]. These linear features are not a surface phenomenon because they have been observed in all the randomly chosen pieces of the parent button.

There are a few locations on the sample surface where these linear features are present in adjacent grains as seen in figure 1(b). For clarity, we have marked the grain boundary in figure 1(b) in white. In these adjacent grains the directionalities of the linear features are different from one another as also observed by Meyers *et al* [11]. The cracks however do not have any effect on the directionality of the pattern.

We further note that the linear features are seen with uniform density wherever they are present. Also the individual lines of each crossed pattern appear with almost equal intensity. This finding is important when we compare the microstructure of the cycled sample with that of the as-cast sample.

[5] A pattern made up of rows of parallel lines which in any two adjacent rows slope in opposite directions (http://www.webster.com: Merriam-Webster Incorporated).

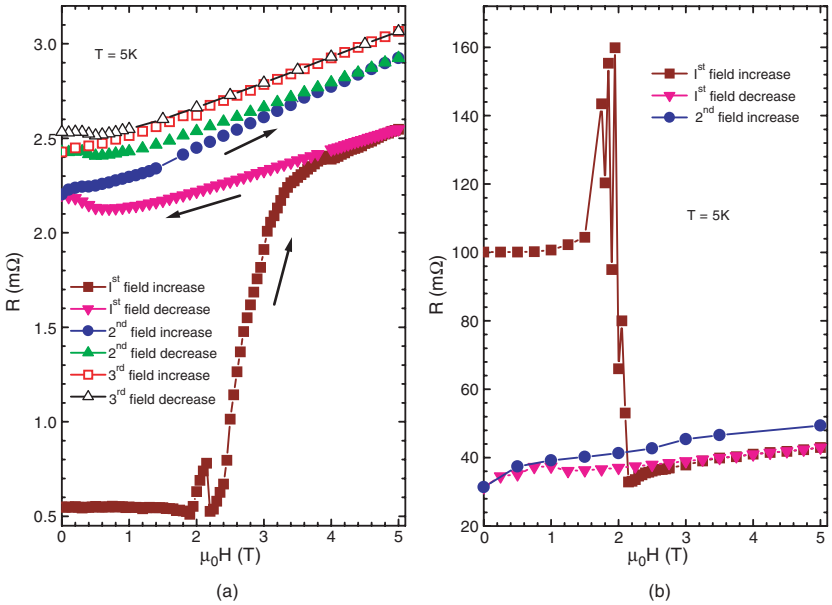

Figure 2. Effect of cycling on the electrical resistance as a function of field at $T = 5$ K. Measurements were performed starting from a ZFC state. (a) Resistance as a function of field at $T = 5$ K for the sample that was not previously exposed to any field or temperature cycle which would cause the FOMST. (b) Resistance as a function of field at $T = 5$ K for the sample that was previously exposed to approximately 25 cycles through the FOMST during other measurements.

Etching was stopped at a stage when no new features were revealed and the surface corrosion was significant. The sample was gently re-polished to remove the colouration and corrosion products and then mounted for electrical resistivity measurements.

3.2. Representative magneto-transport results

Figure 2 compares R versus H curves obtained at 5 K after passing the sample through different numbers of cycles through the FOMST. Both measurements were made starting from a zero-field-cooled (ZFC) state. Each data point was recorded after stabilizing the field. The results shown in figure 2(a) are obtained using a virgin sample that has not undergone any field or temperature cycling which would cause the first order transition. The result shown in figure 2(a) indicates that the AFM Gd_5Ge_4 undergoes a metamagnetic transition to the FM state, which when the field is reduced to $H = 0$, does not revert to the AFM phase [21, 23, 24]. Upon subsequent magnetic cycles the specimen remains essentially in the FM state, although recent x-ray data indicate that a small fraction of the AFM state remains un-transformed [5].

Figure 2(b) shows R versus H curves obtained after cycling the sample (≈25 times) through the FOMST during different measurements. Apart from the rise in the residual resistance value, the contrast between the two results is quite striking. When the sample has not been subjected to any prior field and/or temperature cycling through FOMST the resistance of the FM phase is greater than that of the AFM phase (see figure 2(a)), whereas in figure 2(b) the resistance in the AFM phase exceeds that of the FM phase. Spikes across the transition in this alloy system are believed to be related to unusual dynamics of the magneto-structural transition [17, 25, 26].

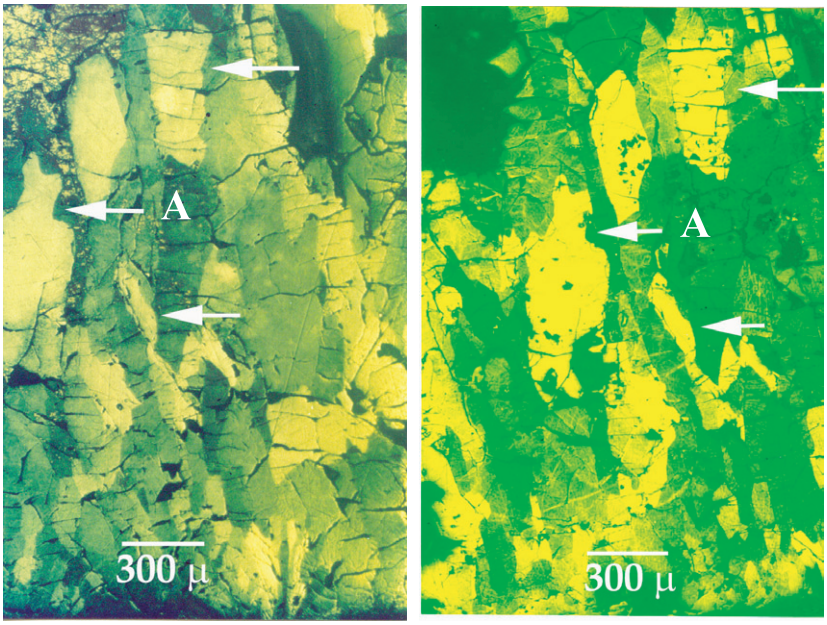

(a) (b)

Figure 3. Optical metallography of the Gd_5Ge_4 sample comparing the grain structure before and after cycling through FOMST. The arrows are used to identify positions on the surface of the sample. (a) Grain structure before cycling through FOMST. (b) Grain structure after cycling the sample repeatedly through the FOMST. The herringbone pattern is visible at length scales much smaller compared to the length scale shown in the figure and thus cannot be seen here.

The result of figure 2 indicates that probably a more dominant mechanism than simple opening of microcracks takes place when the sample undergoes repeated cycling through the FOMST. The contribution to resistivity due to microcracks always being additive does not explain the change of magnetic field dependence of resistance across the transition. A change in behaviour of temperature dependent resistivity has been observed in Si doped Gd_5Ge_4 alloys [14, 16]. This change in behaviour was thought to arise due to change in microstructure as well as change in the atomic configuration [14], i.e. a redistribution of Si and Ge atoms on the intra- and inter-layer sites. We later discuss one of the possible scenarios which explains the results shown in figure 2.

3.3. Microstructure of the sample exposed to temperature and field cycling

Figure 3(b) shows the grain structure and the crack pattern of the sample subjected to field and temperature cycling. For comparison, we show the grain structure of the sample in the as-cast condition in figure 3(a). The arrows in both figures point to identical portions of the sample. We note that the grain structure of the sample subjected to field and temperature cycling is preserved compared to the as-cast sample. Contrary to the expectation, we do not see any drastic change in the crack network at least on the length scale shown in figure 3. In fact the crack pattern remains so much like the network in the as-cast case, that we can actually identify individual cracks (see for example the portion of the sample near the arrow marked 'A'). The only difference that is visible on the surfaces corresponding to both cases is that some small particles were dislodged from the cycled sample, resulting in creation of voids. The dimensions

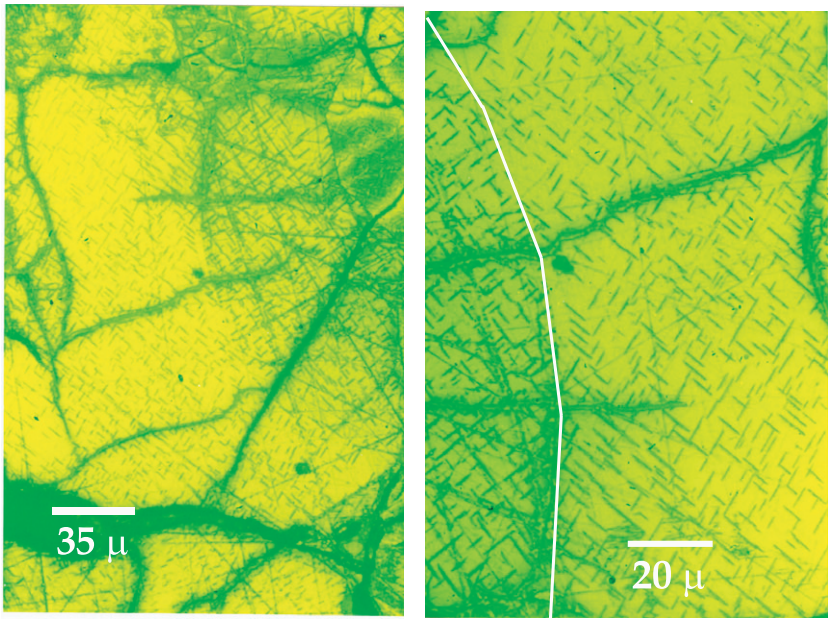

Figure 4. Optical metallography revealing the criss-cross pattern after repeated cycling through the FOMST seen at two different magnifications at about the same location of the Gd_5Ge_4 sample. (a) Criss-cross pattern seen in a region of sample which has a relatively high density of the pattern. (b) Criss-cross pattern in adjacent grains.

of voids range from approximately 20 μm $\times$ 20 μm (the smallest black spots) to slightly more than 500 μm $\times$ 500 μm (the biggest void in the top left corner of figure 3(b)). This comparison shows that if there is some change in the crack pattern after the sample is cycled through the FOMST, that change occurs at a length scale smaller than 20 μm. Also, figure 3 shows that the sample gets more and more brittle as it is subjected to numerous cycles through the FOMST. Breaking of the Si doped Gd_5Ge_4 specimen has been observed by Sousa *et al* [16] after cycling through FOMST.

Observing the sample at a length scale smaller than the one shown in figure 3, we see that the herringbone pattern appears in only a few isolated regions of the sample. Figure 4 shows one location of the sample where the density of this pattern is the highest. This finding is quite opposite to the observation shown in figure 1. In the case of the as-cast sample the herringbone pattern appears almost all over the sample and there are a very few spots (like the left corner of figure 1(a)) where the pattern is absent. Whereas in the case of the sample subjected to repeated field and temperature cycling, the herringbone pattern appears in only a few spots and most of the sample does not show any presence of the pattern. Another observation in the cycled sample is that in those places of the sample where the linear features are present, the density of this pattern has been reduced drastically compared to the density seen in the as-cast condition. Comparing figures 4(a) and 1 (which show the sample at the same length scale) we note that the criss-cross pattern of the cycled sample has been diminished to a large extent. The thickness of individual lines also has clearly decreased. Figure 4(b) shows a smaller portion of the sample which is nearby the location shown in figure 4(a). Here again we can see that the directionality of the criss-cross pattern changes across a grain boundary as was seen in figure 1(b).

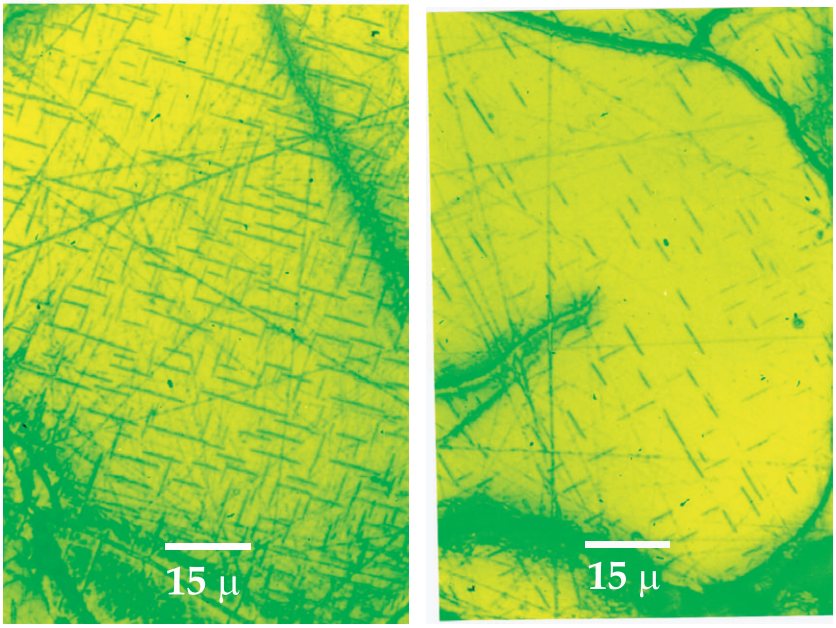

(a) (b)

Figure 5. Optical metallography revealing mostly unidirectional pattern seen at two different locations of the Gd_5Ge_4 sample. The lines in the other direction appear with much lower intensity. (a) Lines mostly in one direction in a high density region. (b) Lines mostly in one direction in a low density region.

Figure 5 shows the herringbone pattern observed in two different regions of the sample, one where the density of the pattern is reasonably high and another where the density is quite low. In both figures it is seen that the individual lines of the criss-cross are more prominent in only one direction. The lines in the other direction are either less intense (as in figure 5(a)) or altogether absent in some places (as in figure 5(b)). This observation is in sharp contrast with figure 1, where the lines of the criss-cross pattern appear with equal intensity in both the directions. We thus see that cycling through the FOMST causes a change in the morphology and density of the herringbone pattern over a length scale of few tens of microns.

3.4. Training effects in magnetization

Through an independent measurement of magnetization as a function of field and temperature on a different and smaller piece (irregularly shaped, less than 0.5 mm^3) of the parent button, we have also observed a training effect in the magnetic properties. The magnetization of any sample should (intuitively) be unrelated to the cracks present in the sample. An effect of repeated cycling through the FOMST on magnetization would mean that some additional phenomenon is taking place in the sample apart from a simple opening of microcracks.

Both isothermal and temperature dependent measurements were made to check for the effect of cycling. The transitions occurring in Gd_5Ge_4 are quite complex in nature and may be irreversible, partially reversible or completely reversible depending on the temperature and field values [20–23]. Thus for simplicity (though not strictly correct), during any isothermal measurement we treat the magnetic field sweep from 0 to 5 T and back to 0 as one cycle

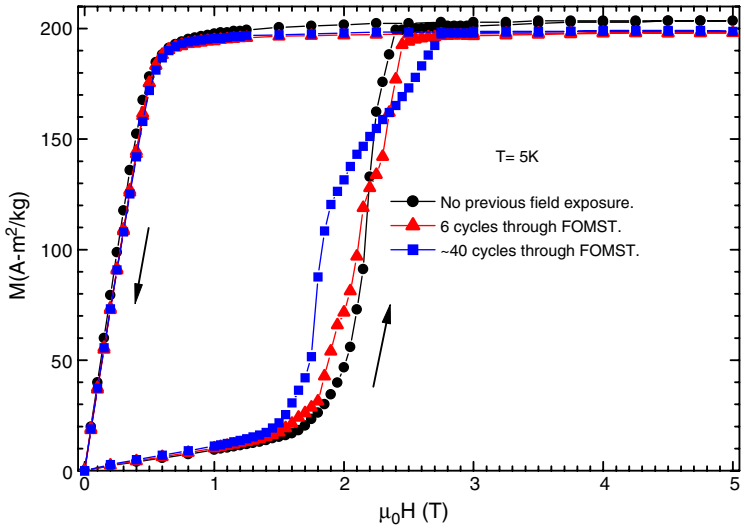

Figure 6. Effect of repeated cycling during various experiments through the magneto-structural transition of Gd_5Ge_4 on the isothermal magnetization behaviour at 5 K. Measurements were performed starting from a ZFC state.

through the FOMST. Similarly, in temperature dependent measurements, we treat one ZFC and field-cooled (FC) measurement together as one cycle. Figure 6 shows the isothermal magnetization as a function of field at $T = 5$ K. In the as-cast case, the magnetization shows a sharp transition from the AFM to FM phase. As the number of cycles increases, the onset field of the metamagnetic transition is lowered and by about 40 such cycles the onset field decreases by about 0.4 T. There is also one more visible change in the behaviour of the M–H curve. In the as-cast sample, the M–H curve shows almost no step-like features across the transition. As the number of cycles increases, small step-like features start appearing across the transition. After a large number of cycles, the curve is divided in two distinct sections: a sharp jump followed by a smoothly varying curve.

At 35 K (see figure 7) the onset field of the AFM–FM transition changes only slightly, whereas the onset field of the FM–AFM transition changes quite significantly between 2 and 15 cycles, and then hardly changes for more cycles. This leads to a situation where the width of hysteresis across the transition depends on the number of temperature and field cycles the sample has been exposed to. Here also a larger number of step-like features in the M–H curve appear across the transition after repeated cycling, a feature similar to that seen at $T = 5$ K.

The changes are also seen in the temperature dependent magnetization measurements. Figure 8 shows the M–T curves obtained in both ZFC and FC protocols at $\mu_0 H = 1.6$ T. In a field of 1.6 T, when the temperature is increased from 5 K, the ZFC sample first undergoes an AFM–FM transition and then an FM–AFM transition [21]. After repeated cycling through the FOMST, the onset temperatures of these transitions change quite appreciably. After about 42 cycles through the FOMST, the M–T curve shows two types of distinct behaviour across the AFM–FM transition which is analogous to the two kinds of behaviour seen across the field induced AFM–FM transition at 5 K (see figure 6). Also the magnetization in the FC curve obtained after 42 cycles is lower at the lowest temperature compared to the magnetization in FC curves obtained after only a few cycles.

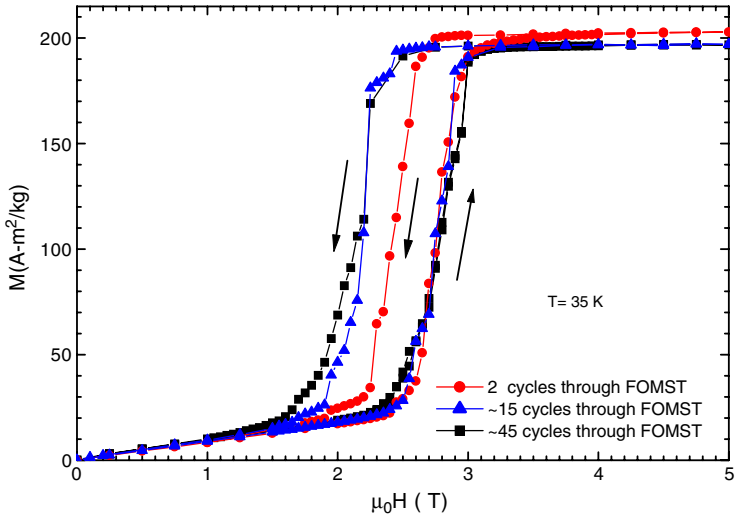

Figure 7. Effect of repeated cycling during various experiments through the magneto-structural transition on the isothermal magnetization behaviour of Gd_5Ge_4 at 35 K. Measurements were performed starting from a ZFC state.

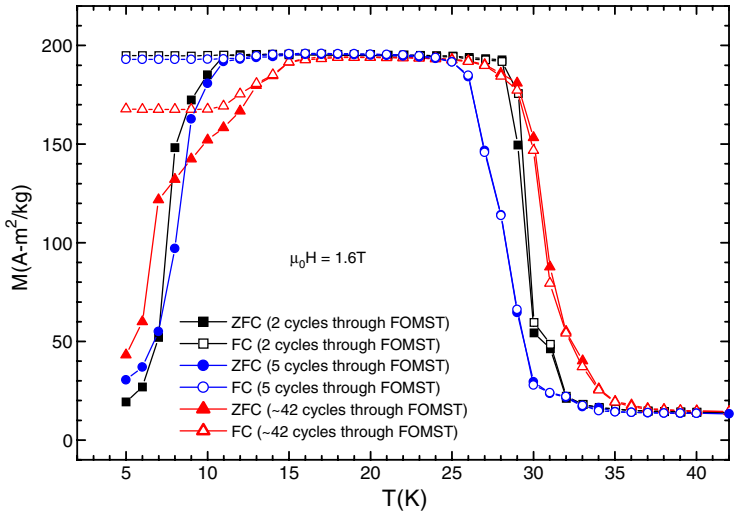

Figure 8. Effect of repeated cycling during various experiments through the magneto-structural transition of Gd_5Ge_4 on the isofield magnetization behaviour at $\mu_0 H = 1.6$ T. All the measurements were performed during warming the sample.

4. Microstructure and training effects

4.1. Origin of the herringbone pattern

We believe that changes in the herringbone pattern as a function of cycling are the key to understanding the training effects observed in magneto-transport and magnetization measurements. But first, we need to discuss what is today's knowledge about the microstructure of Gd_5Ge_4 based alloys.

Szade *et al* [10] concluded that the linear features have a different chemical composition compared to the bulk. The lines contained excess Gd and oxygen. Meyers *et al* [11] and Ugurlu *et al* [12, 13] also concluded through energy dispersive spectroscopy (EDS) studies that the linear features in $Gd_5(Si_xGe_{4-x})$ alloys do have a different chemical composition. We would like to stress here that EDS is not a suitable technique for characterization of Gd_5Ge_4 based alloys, the reason being that the energy of the Ge(Lα) line is 1.188 keV and the energy of the Gd(Mα) line is 1.1843 keV [27]. These two lines are extremely difficult to resolve in a conventional spectrometer and thus any quantitative estimate of the Gd and Ge could lead to unreliable results [28].

Even if we assume that the linear features in Si doped alloys arise due to a chemical composition that contains excess Gd, the situation for the pure compound remains unanswered. The known stable phase of Gd and Ge which has Gd in excess compared to Gd_5Ge_4 is Gd_5Ge_3 [23, 29]. If the herringbone pattern was due to Gd_5Ge_3 (Gd excess), then there would be some regions of the sample which are Gd deficient as the sample was prepared at the stoichiometric Gd_5Ge_4 composition. Also, there would have been some signature of these two phases in magnetization measurements similar to those seen by Magen *et al* [23], but this is not seen in the magnetization measurements performed on the sample used here and thus the possibility of a second, chemically different phase is quite unlikely.

In our understanding, the herringbone pattern may be related to a martensitic transition occurring in Gd_5Ge_4 at low temperatures under applied magnetic field [5] and hydrostatic pressure [22]. When the martensitic phase nucleates in the parent austenite phase, variants of the martensite arrange themselves so that there is no net macroscopic change of shape. This takes place to minimize strain and is known as *self-accommodation* [30]. Patterns similar to Gd_5Ge_4 (though slightly more regular) are also seen in the case of manganites [31]. The similarity of microstructures indicates that a martensitic transition in Gd_5Ge_4 has started well above room temperature and what we observe at room temperature (the O(II) phase) is an intermediate state between the high-temperature zero-field state and the low-temperature high-field state (the O(I) phase). It is quite possible that a precursor to the room-temperature phase occurs during crystallization from melt, as during the crystallization of amorphous $NiZr_2$ [32]. Such precursor phase could be either transient (short lived) or could fall out of equilibrium at some stage of growth and remain kinetically arrested (long lived) [33, 34]. Precursor phenomena are quite commonly seen in martensitic transitions, like in Fe–Pd alloys for example [35]. We conjecture that the following sequence of events takes place during crystallization of Gd_5Ge_4: [melt] $\rightarrow$ [phase having higher symmetry than the orthorhombic O(II) phase] $\rightarrow$ [martensitic transition to the orthorhombic structure O(II) seen at room temperature]. This sequence is quite similar to that seen in $La_{0.33}Ca_{0.67}MnO_3$ [36].

During a solid–solid structural transition, lattice distortion which occurs during the transformation distorts the crystallites (grains) in which this nucleation takes place. In a polycrystalline sample, the surrounding grains obstruct this distortion, thus inhibiting the development of full symmetry of the product phase which leads the material to go into a state of residual stress [37][6]. This stress is normally reduced by twinning the crystallite. We believe that a similar phenomenon of twinning occurs in Gd_5Ge_4, which gives rise to the herringbone pattern seen in figure 1. Gd_5Ge_4 is probably inherently twinned at room temperature. Ugurlu *et al* [12] have shown through their transmission electron microscopy (TEM) studies on $Gd_5Si_2Ge_2$ that the structure of the linear features of the criss-cross pattern is hexagonal and have interpreted these plates as precipitates of a second phase. We however

[6] DoITPoMS Micrograph Library, University of Cambridge, micrograph numbers 663 and 664, http://www.doitpoms.ac.uk/miclib/

note that hexagonal structure can arise at twin boundaries in twinned orthorhombic lattice. The crystal symmetry is still orthorhombic but twinning makes it appear to be hexagonal. This structure is thus known as pseudo-hexagonal and can create confusion about the crystal habit. Such cases are quite well known for certain minerals, like that of Djurleite (orthorhombic–pseudohexagonal) [38], the mineral aragonite ($CaCO_3$) (orthorhombic–pseudohexagonal) [39] and chrysoberyl ($BeAl_2O_4$) (orthorhombic–pseudohexagonal) [40].

We are aware of at least one member of the $Gd_5(Si_xGe_{4-x})$ family of alloys, namely $Gd_5(Si_2Ge_2)$, which shows an intrinsically macroscopic twinned monoclinic structure at room temperature [41]. Similar experiments are now needed on Gd_5Ge_4 to confirm our conjecture.

With this picture in mind we first try to explain the various features of the microstructure and then attempt to explain the training effects in resistivity and magnetization. Our discussion related to the microstructure of Gd_5Ge_4 closely follows the review by Arlt on ferroelectric and ferroelastic ceramics [37].

In our model, Gd_5Ge_4 undergoes a high-temperature martensitic transition on cooling and the O(II) crystal structure seen at room temperature is an intermediate state frozen in time (the martensite has not fully grown). This martensitic transition does not go to a completion even at the lowest temperature in a zero magnetic field or under zero applied pressure. The stable state is the field induced FM state having the O(I) structure. The stable FM Gd_5Ge_4 is generated from the O(II) phase by elongation of the lattice along the '*b*' and '*c*' axes and by contraction along the '*a*' axis [5, 42]. Suppose the nucleation of this stable phase occurs in some grains of the sample. For a grain clamped by other grains in all three directions, twinning can accommodate the strain only along those two directions in which the unit cell length increases. Contraction in the '*a*' direction cannot be compensated, which leads to formation of microcracks, a situation similar to that seen in $YBa_2Cu_3O_7$, where the cracks form due to lack of compensation along the '*c*' axis [37]. Lack of compensation along the '*a*' axis in Gd_5Ge_4 would mean that the cracks should form parallel to the (100) plane. As seen in figure 3 the cracks show a strikingly (almost) parallel pattern in all the grains where they occur. In some of the grains the cracks are not visible, probably due to the '*a*' axis oriented along the plane of the sample. The origin of microcracks discussed above also explains the brittle nature of the sample, an aspect which is extremely important if the material is to be used for technological purposes. The brittle nature of the sample (presence of cracks) can also arise due to large anisotropic linear expansion [42]. But anisotropic expansion alone cannot explain the origin of the herringbone pattern and also the changes of the observed physical properties that take place after numerous cycling.

The microstructure shown in figure 1 is of a section of the sample taken from the interior of the original parent button. In this region of the sample the grains are clamped in all three dimensions. The herringbone pattern of figure 1 is due to twinning, which arises to relieve this three-dimensional stress (assuming that the process of cutting and polishing does not have any effect on the criss-cross pattern). When this section of the sample is mounted for resistivity measurements, the sample is rigidly glued in only two dimensions and the surface is free. Subjecting this section to repeated cycling through the FOMST would take the sample through a de-twinning and twinning cycle with modified mechanical boundary conditions. The twinning which arises due to modified boundary conditions would thus have a different pattern compared to the original microstructure. This is quite evident when we compare figures 1, 4 and 5. Cycling a martensite through the structural transition regime in the presence of known external boundary conditions causes the martensitic transition to occur through a unique variant of the product phase. This phenomenon is usually known as *'training'* or *'education'* of the microstructure [43]. This kind of evolutionary behaviour of the microstructure has been seen in the two-way shape memory effect in Cu–Zn–Al alloys [43] and also in Cu–Al–Mn alloys [44], for instance. In our case, the boundary conditions which depend on the manner in which

the specimen is mounted for either resistivity or magnetization measurements are difficult to determine exactly. But they are obviously different compared to the original stress which arises due to clamping of the grains in the polycrystalline button during crystallization from the melt. We thus see that the microstructure of Gd_5Ge_4 can be trained by passing it through repeated cycles through the FOMST.

The structural transition from the low-field O(II) phase to the high-field O(I) phase occurs by elongation along the '*b*' and '*c*' axes and contraction along the '*a*' axis. Thus when the sample goes from the O(II) phase to the O(I) phase, the cracks along the (100) plane are expected to widen. Similarly, the width of the cracks would be reduced during back-transformation. This repeated increase and decrease of the crack width would result in dislodging islands of the bulk enclosed by the cracks. This is what we see in figure 3. Newer cracks are probably not seen because there are already enough cracks formed in the virgin sample which provide sufficient space for repeated expansion and contraction of the sample.

4.2. Training effects in resistivity

After suggesting a model explaining the origin of the herringbone pattern and the related training effects, we now proceed to explain the effect of cycling observed in transport measurements. From here onwards we will treat the herringbone pattern as a separate phase and refer to it as the herringbone phase. This approach is justified because it is known that twin boundaries can offer a different scattering cross-section for conduction electrons compared to the sample matrix and other defects [45]. We can thus treat our sample in terms of separated phases: (1) the sample matrix excluding the herringbone pattern and (2) the herringbone phase.

Comparing the microstructure before cycling shown in figure 1 with that after cycling in figures 4 and 5, the density of the herringbone phase has reduced drastically. At the same time the resistance shown in figure 2(b) which corresponds to the microstructures in figures 4 and 5 has increased quite appreciably. If we treat the total resistivity of the sample as a combination of resistivities of both separated phases [46], the combined observation of transport measurements and metallography leads us to the conclusion that the herringbone phase has a lower resistivity than the remaining sample matrix. This is quite analogous to copper [45], where a larger number of twin boundaries leads to the lowering of resistivity of the sample. The result shown in figure 2(a) corresponds to a microstructure practically identical to that shown in figure 1. Thus, the large density of the herringbone phase is responsible for the lower value of resistivity in the AFM phase. The herringbone phase probably gets converted along with the AFM phase to the stable FM phase on application of magnetic field (the FM phase is probably de-twinned similar to the case of $Gd_5Si_2Ge_2$ [41]). The resistivity in the FM phase is therefore more or less the property of a single stable phase. This leads to a situation where the AFM to FM transition shows an increase in resistivity rather than the reduction of resistivity which is expected normally as in doped $CeFe_2$ alloys for example [47–49]. When the density of the herringbone phase reduces after sufficient cycling through the FOMST, the resistivity of the low-field phase is more or less representative of the single AFM phase. In such a situation, the resistivity of the AFM phase should be larger than that of the FM phase. This behaviour is seen in figure 2(b). A change of behaviour of resistivity across the FOMST has earlier been reported in temperature dependent studies in Si doped alloys [14, 16, 17]. A change of microstructure as well as changes at the atomic level were postulated [14] to explain these results. Our results show that a change of microstructure (i.e. a change in the amount and morphology of one of the two competing phases) is probably one of the causes which can explain the rise in resistivity and also the change in magnetic field dependence of resistivity.

The system (or the microstructure) can be probably trained through an incomplete transition as well. This can be seen from the results shown in figure 2, where the AFM to

FM transition is partially incomplete and the back-transformation from FM to AFM does not take place at all. The system still evolves towards a different state after repeated cycling.

4.3. Training effects in magnetization

The sample used in magnetization studies was less than 0.5 mm^3 in size, which is only a few grains, as can be seen from figure 3. The mechanical boundary conditions are obviously quite different for a sample loaded in a SQUID magnetometer and for that loaded for resistivity measurements. As mentioned earlier, twinning may occur to reduce strain and thus to lower the total energy of the system. The number of interfaces created during twinning and the length of each interface depends upon the balance between the increase of interface energy and the decrease of strain energy [30]. Any interface forms an energy barrier between two phases (the low-field AFM and the high-field FM, in this case) and a transition can be caused only when this barrier is surpassed [6] and also when the strain energy is overcome. If magnetic field is applied to cause the transition, then onset of the metamagnetic transition would depend directly on the density of the interfaces and the amount of strain present in the low-field phase. We have seen that the density of the herringbone phase (and thus the density of interfaces) decreases along with some stress relief when the sample is cycled through the FOMST with reduced boundary conditions. A change in the density of the herringbone phase along with the change in strain field would thus imply the change of the onset field of the metamagnetic transition. This is precisely what we observe in figures 6 and 7. A similar argument holds for temperature induced transition and we do see that the onset temperatures of the AFM–FM and the FM–AFM transition change as the sample is repeatedly cycled through the FOMST. A situation where the onset field of the FM phase depends on the amount of cycling through the phase separated state is also reported in the case of CMR perovskite manganites [50]. The distribution of interfaces would probably decide the coherence volume over which nucleation occurs during a phase transition. The behavioural changes in the M–T and M–H curves with cycling shown in figures 6–8 are probably related to the change in coherence volume for nucleation. After about 40 cycles through the FOMST, the M–H curve at 5 K (see figure 6) across the AFM–FM transition is divided into two distinct sections. Earlier, Tang *et al* [21] postulated the presence of two AFM states at low temperatures based on two observations: (1) a sharp jump in a field dependent magnetization followed by a smooth curve and (2) thermomagnetic irreversibility in temperature dependent magnetization seen at low fields. The phase transition between these two AFM phases has not been detected in electrical transport [19] and x-ray diffraction measurements [5, 42]. No evidence of spin canting has been seen in magnetic scattering experiments [51] and there has also been no signature of the AFM1 and AFM2 phases coexisting together [19].

Finally, comparing the magnetization curves in figure 8, we observe that after a large number of cycles the FC curve has lower magnetization values at the lowest temperature than those obtained after only a few cycles. From the FC curves, it appears that the low-temperature AFM state cannot be recovered from the FM state without extensive cycling, after which a small fraction of the AFM phase can be reinstated on cooling. It is quite likely that the back-transformation from the FM to AFM phase is possible only after a sufficient strain relief, which results from exposing the sample repeatedly to magnetic field and temperature cycles. Most probably, residual strain in the sample, and hence the microstructure, play important roles in deciding which transition is irreversible, partially reversible or completely reversible.

5. Conclusion

In conclusion, detailed optical metallography measurements on Gd_5Ge_4 enabled us to correlate changes in microstructure with changes in magneto-transport and magnetization properties.

The possibility of a kinetically arrested phase embedded in a stable room-temperature phase has been discussed. Our results provide an interesting case study to explore the rich phenomenon of nucleation and growth in materials undergoing solid–solid phase transitions. Further studies on single crystals would be more instructive on the dynamics of phase transition in Gd_5Ge_4. The studies of nucleation and growth mechanisms across solid–solid transitions in polycrystalline samples which lead to changes in microstructure and other physical properties, nevertheless, are important, as any bulk material used directly for technological purposes is more likely to be of polycrystalline nature.

Acknowledgments

We thank Dr A O Tsokol for providing the sample of Gd_5Ge_4. Work at Ames Laboratory is supported by the Office of Basic Energy Sciences, Materials Sciences Division of the US Department of Energy, under contract No W-7405-ENG-82 with Iowa State University. We also thank Dr S B Roy and Dr P Chaddah for useful discussion.

References

[1] Pecharsky V K and Gschneidner K A Jr 2001 *Adv. Mater.* **13** 683
[2] Pecharsky V K and Gschneidner K A Jr 1997 *J. Alloys Compounds* **260** 98
[3] Morellon L, Blasco J, Algarabel P A and Ibarra M R 2000 *Phys. Rev.* B **62** 1022 and references cited there in
[4] Pecharsky A O, Gschneidner K A Jr, Pecharsky V K and Schindler C E 2002 *J. Alloys Compounds* **338** 126
[5] Pecharsky V K, Holm A P, Gschneidner K A Jr and Rink R 2003 *Phys. Rev. Lett.* **91** 197204
[6] Imry Y and Wortis M 1979 *Phys. Rev.* B **19** 3580
[7] Gschneidner K A Jr, Pecharsky A O, Pecharsky V K, Lograsso T A and Schlagel D L 2000 *Rare Earth and Actinides: Science, Technology and Applications IV* ed R G Bautista and B Mishra, (Warrandale, PA: Minerals Metals and Materials Society) p 63
[8] Pecharsky A O, Gschneidner K A Jr and Pecharsky V K 2003 *J. Appl. Phys.* **93** 4722
[9] Han M, Jiles D C, Snyder J E, Lo C C H, Leib J S, Paulsen J A and Pecharsky A O 2003 *J. Appl. Phys.* **93** 8486
[10] Szade J, Skorek G and Winiarski A 1999 *J. Cryst. Growth* **205** 289
[11] Meyers J S, Chumbley L S, Laabs F and Pecharsky A O 2002 *Scr. Mater.* **47** 509
[12] Ugurlu O, Chumbley L S, Schlagel D L and Lograsso T A 2005 *Acta Mater.* **53** 3525
[13] Ugurlu O, Chumbley L S, Schlagel D L, Lograsso T A and Tsokol A O 2005 *Scr. Mater.* **53** 373
[14] Levin E M, Pecharsky V K, Gschneidner K A Jr and Miller G J 2001 *Phys. Rev.* B **63** 064426
[15] Levin E M, Pecharsky V K, Gschneidner K A Jr and Miller G J 2001 *Phys. Rev.* B **64** 235103
[16] Sousa J B, Braga M E, Correia F C and Carpinteiro F 2003 *Phys. Rev.* B **67** 134416
[17] Sousa J B, Pereira A M, Correia F C, Teixeira J M, Araújo J P, Pinto R P, Braga M E, Morellon L, Algarabel P A, Magen C and Ibarra M R 2005 *J. Phys.: Condens. Matter* **17** 2461
[18] Pérez-Reche F, Casanova F, Vives E, Mañosa L, Planes A, Marcos J, Batlle X and Labarta A 2006 *Phys. Rev.* B **73** 014110
[19] Chattopadhyay M K, Manekar M A, Pecharsky A O, Pecharsky V K, Gschneidner K A Jr, Moore J, Perkins G K, Bugoslavsky Y V, Roy S B, Chaddah P and Cohen L F 2005 unpublished
[20] Levin E M, Gschneidner K A Jr and Pecharsky V K 2002 *Phys. Rev.* B **65** 214427
[21] Tang H, Pecharsky V K, Gschneidner K A Jr and Pecharsky A O 2004 *Phys. Rev.* B **69** 064410
[22] Magen C, Arnold Z, Morellon L, Skorokhod Y, Algarabel P A, Ibarra M R and Kamarad J 2003 *Phys. Rev. Lett.* **91** 207202
[23] Magen C, Morellon L, Algarabel P A, Marquina C and Ibarra M R 2003 *J. Phys.: Condens. Matter* **15** 2389
[24] Chattopadhyay M K, Manekar M A, Pecharsky A O, Pecharsky V K, Gschneidner K A Jr, Moore J, Perkins G K, Bugoslavsky Y V, Roy S B, Chaddah P and Cohen L F 2004 *Phys. Rev.* B **70** 214421
[25] Casanova F, Labarta A and Batlle X 2005 *Phys. Rev.* B **72** 172402
[26] Casanova F, Labarta A, Batlle X, Vives E, Marcos J, Manosa L and Planes A 2004 *Eur. Phys. J.* B **40** 427
[27] Robinson J W 1991 *Practical Handbook of Spectroscopy* (Boca Raton, FL: CRC Press)
[28] Gama S, Alves C S, Coelho A A, Ribeiro C A, Persiano A I C and Silva D 2004 *J. Magn. Magn. Mater.* **272–276** 848

[29] Holtzberg F, Gambino R J and McGuire T R 1967 *J. Phys. Chem. Solids* **28** 2283
[30] Bhattacharya K 2003 *Microstructure of Martensite: Why it Forms and How it Gives Rise to the Shape Memory Effect* (New York: Oxford University Press)
[31] Podzorov V, Kim B G, Kiryukhin V, Gershenson M E and Cheong S W 2001 *Phys. Rev.* B **64** 140406
[32] Sutton M, Yang Y S, Mainville J, Jordan-Sweet J L, Ludwig K F and Stephenson G B 1989 *Phys. Rev. Lett.* **62** 288
[33] Sirota E B and Herhold A B 1999 *Science* **283** 529
[34] Kartha S, Krumhansl J A, Sethna J P and Wickham L K 1995 *Phys. Rev.* B **52** 803
[35] Seto H, Noda Y and Yamada Y 1990 *J. Phys. Soc. Japan* **59** 978
[36] Wang R, Gui J, Zhu Y and Moodenbaugh A R 2001 *Phys. Rev.* B **63** 144106
[37] Arlt G 1990 *J. Mater. Sci.* **25** 2655
[38] http://www.cryst.chem.uu.nl/lutz/twin/djurleite_hex.html
[39] http://mineral.galleries.com/minerals/carbonat/aragonit/aragonit.htm
[40] http://mineral.galleries.com/minerals/oxides/chrysobe/chrysobe.htm
[41] Choe W, Pecharsky V K, Pecharsky A O, Gschneidner K A Jr, Young V G and Miller G J 2000 *Phys. Rev. Lett.* **84** 4617
[42] Mudryk Y, Holm A P, Gschneidner K A Jr and Pecharsky V K 2005 *Phys. Rev.* B **72** 064442
[43] Lovey F C and Torra V 1999 *Prog. Mater. Sci.* **44** 189
[44] Pérez-Reche F, Stipcich M, Vives E, Mañosa L, Planes A and Morin M 2004 *Phys. Rev.* B **69** 064101
[45] Lu L, Shen Y, Chen X, Qian L and Lu K 2004 *Science* **304** 422
[46] Rossiter P L 1991 *The Electrical Resistivity of Metals and Alloys* (Cambridge: Cambridge University Press)
[47] Singh K J, Chaudhary S, Chattopadhyay M K, Manekar M A, Roy S B and Chaddah P 2002 *Phys. Rev.* B **65** 094419
[48] Manekar M, Chaudhary S, Chattopadhyay M K, Singh K J, Roy S B and Chaddah P 2001 *Phys. Rev.* B **64** 104416
[49] Manekar M, Chaudhary S, Chattopadhyay M K, Singh K J, Roy S B and Chaddah P 2002 *J. Phys.: Condens. Matter* **14** 4477
[50] Zhu D, Hardy V, Maignan A and Raveau B 2004 *J. Phys.: Condens. Matter* **16** L101
[51] Tan L, Kim J W, Goldman A I, McQueeney R J, Wermeille D, Sieve B, Lograsso T A, Schlagel D L, Budko S L, Pecharsky V K and Gschneidner K A Jr 2005 *Phys. Rev.* B **71** 214408